On slip effect in free coating of non-Newtonian fluids*)

A. Dutta and R. A. Mashelkar

Chemical Engineering Division, National Chemical Laboratory, Pune (India)

Abstract: The failure of the current theories to predict the coating thickness of non-Newtonian fluids in free coating operations is shown to be a result of the effective slip at the moving rigid surface being coated. This slip phenomenon is a consequence of stress induced diffusion occurring in flow of structured liquids in non-homogeneous flow fields. Literature data have been analysed to substantiate the slip hypothesis proposed in this work. The experimentally observed coating thickness is shown to lie between an upper bound, which is estimated by a no-slip condition for homogeneous solution and a lower bound, which is estimated by using solvent properties. Some design considerations have been provided, which will serve as useful guidelines for estimating coating thickness in industrial practice.

Key words: Slip, free coating, non-Newtonian fluid

Notation

a	exponent in eq. (15)
b	$n/(4 - n)(n + 1)$
Ca	Capillary number
D	diffusivity
De	Deborah number
g	acceleration due to gravity
G	Goucher number
h	thickness profile
h_0	final coating thickness
K	consistency index
L	length available for diffusion
L_t	tube length
n	power-law index
ΔP	pressure drop
Q	flow rate
R	cylinder radius
R_t	tube radius
t	time available for diffusion
T_0	dimensionless thickness without slip
T_s	dimensionless thickness with slip
U_c	theoretically calculated withdrawal velocity to match the film thickness
u_s	slip velocity
U	withdrawal velocity
U_w	theoretically calculated withdrawal velocity based on solvent properties
U^*	effective withdrawal velocity
x	distance in the direction of flow
y	distance transverse to the flow direction
α	curvature coefficient
β	slip coefficient
δ	curvature coefficient
Δ	rate of deformation tensor
θ	u_s/U
λ	relaxation time
ρ	density
σ	surface tension
σ'	shear stress in tube flow
σ_w	wall shear stress in tube flow
τ	stress tensor
τ_w	wall shear stress
ϕ	T_s/T_0

1. Introduction

Vertical withdrawal of a surface from a quiescent pool of liquid results in adherence of a liquid film on to the surface. The coating technique based on this principle is known as free coating, where the surface to be coated is initially immersed in a bath of coating liquid and then withdrawn continuously. In industrial applications, the free coating process is commonly used to apply a large variety of coating formulations onto solid substrates like wires, fibres, papers, plastic films, metal foils etc. The particular combination of substrate and coating liquid, however, is governed by the end use of the coated product. Owing to its con-

siderable practical importance, a detailed scientific understanding of the free coating mechanism is necessary. In particular, a sound knowledge regarding the relationship between the final coating thickness, withdrawal speed and the fluid properties is essential for effective design, optimal control, and efficient operation of the free coating process.
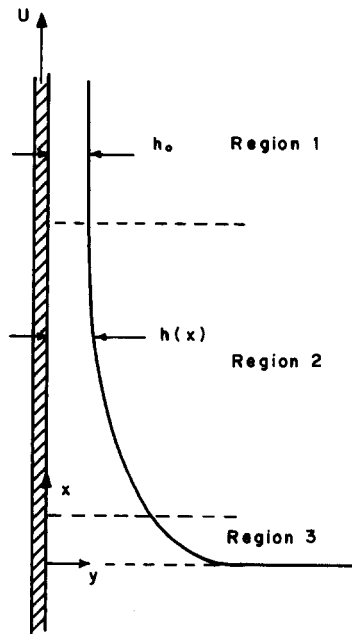

Fig. 1. Schematic representation of the flow situation considered for free coating analysis

Following the work of Landau and Levich [1] a number of theories have been developed to predict coating thickness as a function of process and operational variables. Figure 1 shows the geometry of a model that is commonly used. A flat sheet is withdrawn vertically at a speed U from a liquid bath, whose free surface is at $x = 0$. A dynamic equilibrium between the force of gravity and the viscous drag on the sheet leads to a constant coating thickness h_0 in the region 1, which is somewhat removed from the free surface. In region 3, which is nearest to the free surface, the effects of surface tension are usually assumed to be dominant in comparison to viscous and gravitational forces. In region 2, the final profile of the free surface is established as a result of the interaction of viscous, gravitational and interfacial forces. The inertial effects assume importance at higher speeds. A number of theories applicable for Newtonian liquids have been developed in the literature, which, in recent times have incorporated improved approximations concerning gravitational, inertial

forces etc. [2 – 5]. Since coating formulations are invariably dispersed systems, they do exhibit non-Newtonian behaviour as well. Therefore, there has been a considerable effort to develop theories for non-Newtonian liquids [6 – 12]. A variety of models such as Ostwald-deWaele power-law model [6 – 8], Ellis model [9 – 11], Bingham model [10] etc. have been used.

In spite of the very large effort that has gone in to the development of models for predicting coating thickness for non-Newtonian fluids, there has been no agreement between the experimental observations and theoretical predictions of the various models. Indeed, it is interesting to find that the experimentally observed values of coating thickness with non-Newtonian fluids have been always much less than those predicted by the theory. This is somewhat surprising, especially in view of the fact that the theories appear to work perfectly for Newtonian fluids, but they fail rather badly even when mildly non-Newtonian fluids are encountered. In the present paper we shall be focussing attention on this important phenomenon and presenting a possible hypothesis to explain this discrepancy.

2. Previous experimental observations

In order to see the sort of difference which currently exists between theory and practice, it is useful to cite some typical data in the literature. Normally, the coating thickness depends upon the density (ρ), gravity (g), the surface tension (σ), the withdrawal velocity (U) and the rheological properties. Assuming that the fluid under consideration obeys an Ostwald-deWaele power law behaviour

$$\tau = -K(\varDelta : \varDelta)^{(n-1)/2} \varDelta \tag{1}$$

the following non-dimensional parameters are introduced to define a normalised film thickness (T_0) and a capillary number (Ca)

$$T_0 = h_0 \left(\frac{\rho g}{K U^n}\right)^{1/(n+1)}, \quad Ca = \frac{K h^{1-n} U^n}{\sigma}. \tag{2}$$

In figure 2, we have shown the normalised coating thickness as a function of the capillary number in the case of the data obtained by Gutfinger [13]. The data are compared with the theoretical results obtained by Gutfinger and Tallmadge [6] who have developed theories to predict the coating thickness of power-law
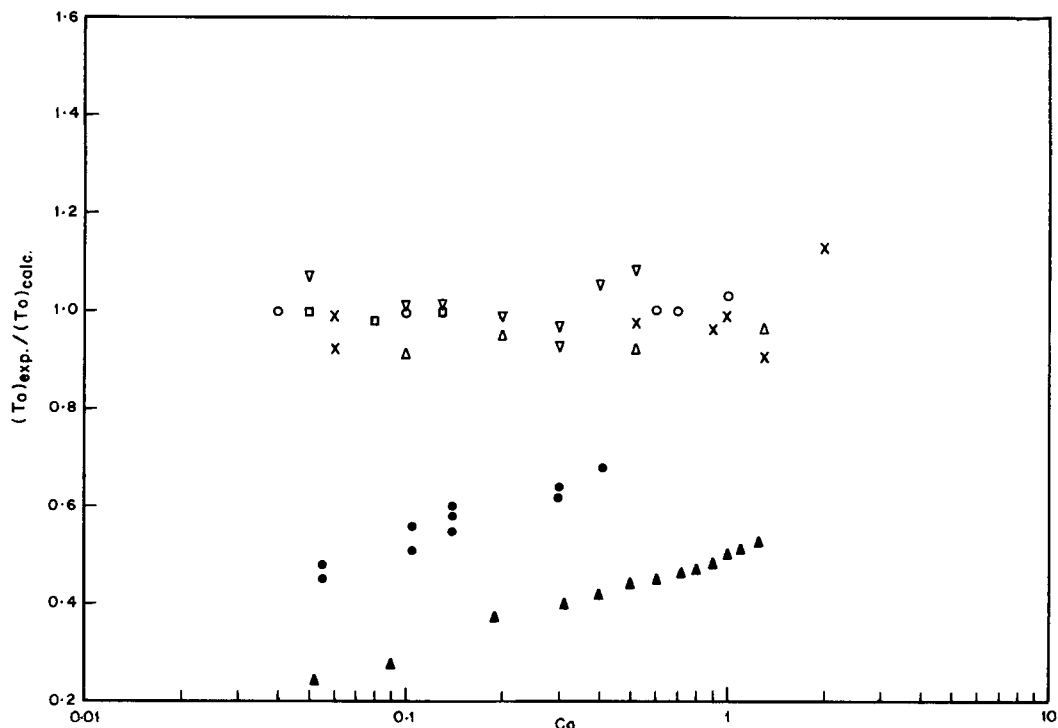
Fig. 2. Comparison of experimental and calculated coating thicknesses for plate withdrawal [6]. Newtonian: (O) Glycerine; (△), (▽), (□) Glycerine-water; (×) Mineral oil. Non-Newtonian: (●) 0.16% Carbopol (▲) 0.2% Carbopol solution in water

fluids. The theoretical results by Gutfinger and Tallmadge are given for low capillary numbers as

$$T_0 = \left[\frac{\alpha^2}{2}\left(\frac{2n+1}{n}\right)^{4n/3}\right]^{1/(n+1)} Ca^{1/(3(n+1))} \qquad (3)$$

and for the general case as

$$T_0 = \left[\frac{\delta^6(2n+1)^4}{8} Ca\right]^{n/(4-n)(n+1)}$$

$$\cdot [1 - T_0^{(n+1)/n}]^{4n/(4-n)(n+1)} . \qquad (4)$$

Here, α and δ are the curvature coefficients, which have been shown in table 1 for different power-law indices. For Newtonian fluids, eqs. (3) and (4) reduce to the form derived by Landau and Levich [1] and White and Tallmadge [2], respectively.

It is seen from these data that whereas for Newtonian liquids the agreement between the theory and

the experiments is very good, the theory overpredicts the coating thickness in the case of non-Newtonian liquids. In most cases, the data presented by Spiers et al. [10], which are not presented here, show exactly the same trend in the sense that the observed coating thickness lies appreciably below their predictions of the "improved" power-law theory.

There have been some experimental reports in the literature pertaining to wire coating by withdrawal from non-Newtonian fluid baths. The data by Roy [14] and Middleman [16, 17] on wire coating show that again the theoretical predictions lie way above the experimentally observed coating thickness. In cylinder withdrawal, the film thickness T_0 depends on an additional parameter, the Goucher number, defined as

$$G = R\left(\frac{\rho g}{2\sigma}\right)^{1/2} .$$

Table 1. Curvature coefficients for power-law liquids [6]

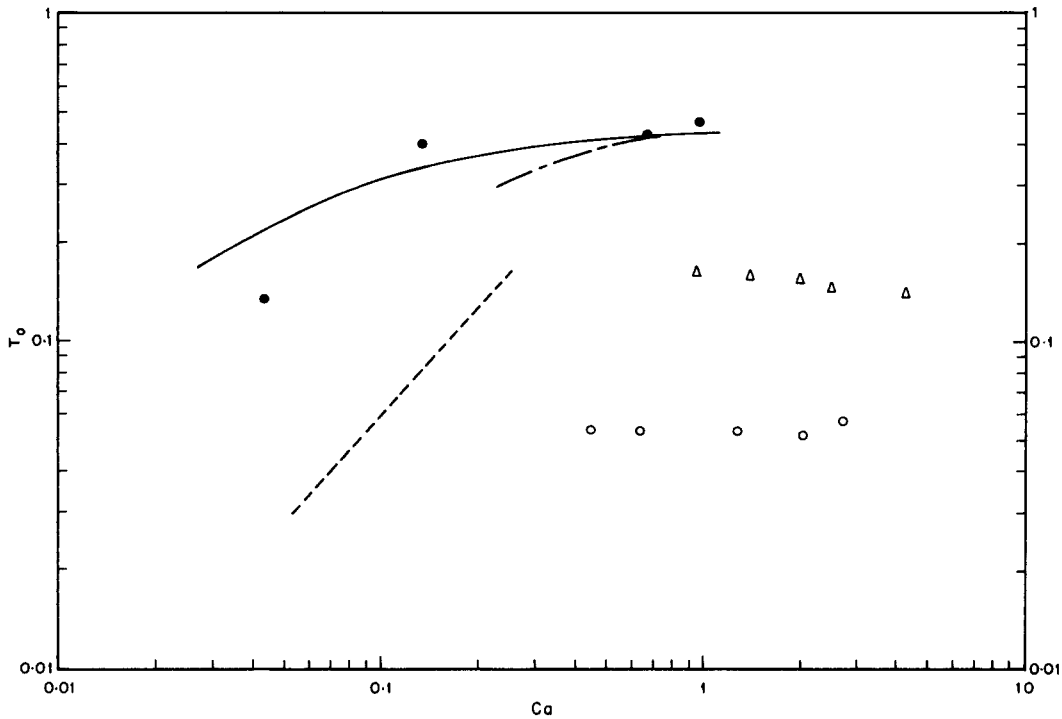| n	1	0.9	0.8	0.7	0.6	0.5	0.4	0.3	0.2
α	0.643	0.720	0.809	0.910	1.028	1.164	1.324	1.514	1.742
δ	0.643	0.727	0.837	0.987	1.210	1.560	2.270	4.410	30.50

Fig. 3. Comparison of experimental and theoretical results for cylinder withdrawal [14]. Mineral oil (Newtonian): (●) Experiment; ——— Calc., G = 0.173. 0.5% Aqueous carbopol 934 solution: (○) Experiment; – – – Calculated, G = 0.121. 0.5% Aqueous carbopol 941 solution: (△) Experimental, — — — Calculated, G = 0.119

In figure 3 we show the experimental data obtained by Roy [14] compared with the theoretical predictions obtained on the basis of Tallmadge theory [15]. Again, one observes a fairly good agreement with data obtained with Newtonian fluids, but the experimental data for non-Newtonian fluids are in serious disagreement with the corresponding theoretical predictions.

In order to explain such a discrepancy, Middleman [16] as well as Spiers et al. [10] conjectured that the differences between the experimental results and the theoretical predictions are probably due to viscoelasticity. The qualitative arguments used by Middleman [16, 17] focussed attention on the possible alterations that viscoelasticity might bring in the free surface behaviour in region 3 shown in figure 1. He argued that these are essentially large Deborah number flows. He calculated the time required for the fluids to accelerate from the relatively quiescent bath through the dynamic meniscus region by arguing that the order of magnitude of the distance traversed would be roughly equal to the height of meniscus which is of the order of $(\sigma/\rho g)^{1/2}$. With a withdrawal velocity of U the time to move this distance would be in the

neighbourhood of $(\sigma/\rho g)^{1/2}/U$. Therefore a Deborah number defined as

$$De = \frac{\lambda U}{\left(\dfrac{\sigma}{\rho g}\right)^{1/2}} \qquad (5)$$

would approach values of unity and more. Here λ is the relaxation time of the viscoelastic fluid under consideration. He argued that since large Deborah number flows are dominated by elastic forces, the fluid would respond more like an elastic solid than a viscous fluid. This would suggest that little viscous entrainment of liquid would occur and therefore the coating thickness would be reduced.

Although intuitively appealing, such an argument leaves much to be desired. For instance, this argument does not explain the reduced entrainment for carbopol 934 solutions which have been observed to possess no detectible elastic properties by Roy [14] and Gutfinger [13]. In fact, we shall show later that the difference between the experimental and calculated values for carbopol 934 solution is an order of

magnitude higher than that obtained for more elastic carbopol 941 solutions. Additionally, viscoelasticity should play a more dominant role as shear rate increases, which in turn implies that the magnitude of the discrepancy should increase as the withdrawal velocity is increased. Experimental observations, however, exhibit no such trend. In fact, experimental data [16, 17] indicate that large differences between calculated and measured film thicknesses exist even when the Deborah number is rather small.

The above arguments suggest that we must look for an alternative explanation of the phenomenon of entrainment reduction. We propose that this phenomenon is most likely to be due to a slip which occurs at the solid-liquid interface. The causes and the consequences of this phenomenon will be discussed comprehensively in what follows.

3. Slip hypothesis

A considerable evidence is mounting in recent years, which shows that the no-slip condition conventionally and conveniently used to solve hydrodynamic problems may no more be valid when inhomogeneous flows of structured fluids such as polymer solutions, polymer melts or suspensions are encountered. Large experimental evidence [18 – 21] existing in the literature shows that this may occur in many systems; but the most dramatic effects are likely to occur when the channel dimensions (or transverse dimensions) are rather small and the channel lengths (or distances in the axial direction) are rather large. For instance, the effects are most predominant in very narrow bore capillaries (say, less than 1 mm dia) or in freely falling films (see Astarita et al. [18], Carreau et al. [19]). Indeed, if the phenomenon of slip occurs in freely falling films, where the thicknesses are of the order $10^{-2} - 10^{-1}$ cm and lengths are of the order of $5 - 10$ cm, then it is most likely to occur in free coating phenomenon described in region 1 in figure 1, where typically, the thicknesses are rather small and the lengths are orders of magnitude higher than those encountered in freely falling films.

In the case of withdrawal of polymer solutions from a bath, it can be qualitatively seen that a slippage at the surface would imply a reduced entrainment velocity for the fluid. Thus, if the withdrawal velocity is U and slip velocity is u_s, then the effective velocity with which the fluid will be withdrawn would be $U - u_s$. Such a reduction in effective entrainment velocity will reduce the coating thickness as well. We shall develop this qualitative argument semi-quantitatively now.

4. Approximate estimate of solvent-layer thickness in free coating

With special reference to macromolecular solutions, a thermodynamic analysis of macromolecular migration was presented by Metzner et al. [22]. This analysis relies on an observation that in a moving, deforming fluid the dissolved molecules become aligned and stretched, thus changing their entropy and free energy levels. In any flow process in which the stress or the strain rate levels vary with position within the fluid, the macromolecular orientation and extension, and consequently the free energy, will also vary with the position. In order that the free energy becomes independent of position at steady state, compensating concentration gradients are induced. The net result is to cause the macromolecules to migrate towards regions of lower stress levels.

The arguments by Tirrell and Malone [23] are qualitatively similar. Metzner et al. [22] have presented an analysis which pertains to the calculation of rate of unsteady diffusion of polymer molecules from the wall region which amounts to the development of a solvent boundary layer which is position dependent. Metzner et al. were able to use this simple analysis to calculate the extent of slip velocities and they found that these presented reasonable order of magnitude estimates. The arguments presented by Janssen [24] are somewhat different in the sense that he suggested that existence of a diffusion instability creates a wall slip. If such an explanation was to be accepted, then slip effect would appear to occur in relatively short distances. Since Metzner's approach places more stringent restrictions on the development of a solvent layer in the neighbourhood of a solid wall, it will be useful to pursue this argument further.

Let us consider the migration of macromolecules away from the wall, occurring as a transient molecular diffusion process. When the macromolecules migrate from the surface, there will be a concentration depletion at the wall and a layer which has a considerably less concentration of macromolecules will be created. The location at which this concentration is appreciably different from its initial uniform value can be easily estimated as

$$Y \sim (Dt)^{1/2} \tag{6}$$

where D is the molecular diffusivity of macromolecules and t is the time for the diffusion process. If L is the length over which diffusion has occurred and U^* is the velocity with which the fluid in the neighbour-

hood of the solid surface moves, then the time available for diffusion is given as

$$t \sim \frac{L}{U^*} \tag{7}$$

where U^* is related to the withdrawal velocity U and the slip velocity u_s as

$$U^* = U - u_s. \tag{8}$$

The slip velocity, u_s is conventionally correlated with the wall shear stress as

$$u_s = \beta \tau_w. \tag{9}$$

Substitution of eqs. (7), (8), and (9) in eq. (6) gives

$$y \sim \left(\frac{DL}{U - \beta \tau_w} \right)^{1/2}. \tag{10}$$

In the case under consideration we have

$$\tau_w = \rho g h_0. \tag{11}$$

Combining eqs. (10) and (11) gives:

$$\frac{y}{h_0} \sim \left(\frac{DL/h_0^2}{U - \beta \rho g h_0} \right)^{1/2}. \tag{12}$$

A rough order of magnitude calculation can be done based on the above. Typically the diffusivities of macromolecules in aqueous solutions are in the range of $10^{-6} - 10^{-7}$ cm^2/s [25 – 27]. Coating thicknesses are usually of the order of 10^{-2} cm. The coating lengths (L) used in the experiments as described in the foregoing are of the order of 100 cm. The slip coefficient β depends upon the polymer type and concentration. Based on the analysis of the data by Astarita [18] and Carreau et al. [19], who studied flow of falling films over inclined planes with similar solutions as those used by experimentalists who have measured the coating thicknesses, it is readily seen that β is the of the order of 10^{-2} cm^2 s/g. Since withdrawal velocities are around 10 cm/s, the above values show that we have y/h_0 approaching 0.1 to 0.3; thus indicating that a significant depletion of macromolecules from the wall region takes place. This implies a major slip effect.

5. Coating thickness in the presence of slip effect

In the foregoing we have discussed the possible extent of slip effect in coating operations. If the hypothesis that such slip effects are indeed possible is accepted, then it will be of interest to calculate the dimensionless coating film thickness in the presence of slip.

Fortunately it turns out that the hydrodynamic calculation can be much easier, if a corresponding no-slip calculation for evaluating coating thickness as a function of process and operational variables is available. As indicated earlier, the principal difference between the slip case and the no-slip case is substitution of an effective entrainment velocity given by $U^* = U - u_s$ in place of the withdrawal velocity U. The calculations for any of the existing theories can be easily modified to account for the slip effect. Such a calculation gives a coating thickness in the presence of slip (T_s) in the case of low capillary number as

$$\phi = \frac{T_s}{T_0} = [1 - \theta]^{2n/(2n+1)} \tag{13}$$

and in general form as

$$\phi^{(1 - b(1-n))/4b}(1 - T_0^{(n+1)/n}) = (1 - \theta) - (\phi T_0)^{(n+1)/n} \tag{14}$$

where $b = \dfrac{n}{(4 - n)(n + 1)}$ and $\theta = u_s/U$. It is apparent from eq. (13) that ϕ decreases as the dimensionless slip velocity (θ) increases. Alternatively, as might be expected, slip is always accompanied by a reduction in entrainment as compared to the no-slip situation. Interestingly for low capillary numbers, the ratio ϕ is predicted to be independent of Ca.

Eq. (14) is implicit in ϕ and has to be obtained numerically for given values of θ and T_0 (or Ca). Figures 4 and 5 illustrate some typical results. In particular, the ratio ϕ is shown as a function of slip velocity for different capillary numbers and pseudoplasticity indices, respectively. $\theta = 0$ corresponds to no-slip situation which implies that $\phi = 1$. Similarly, $\theta = 1$ corresponds to complete slip which gives $\phi = 0$. In practical problems $0 < \theta < 1$. The results show that for all cases, a decrease in ϕ is associated with an increase in slip velocity. The variation, however, appears to be a relatively weak function of Ca and moderately strong function of the pseudoplasticity index, n. Besides, it is evident that the predictions obtained from the general eq. (13) and from eq. (14) are quite close for small values of Ca.
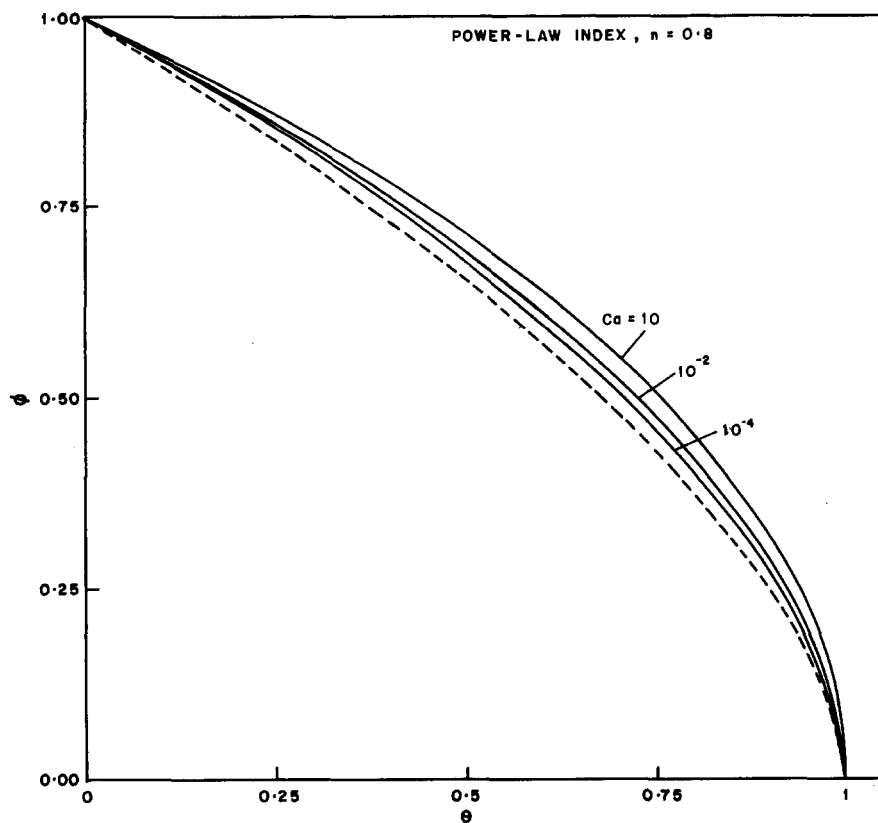
Fig. 4. Effect of slip velocity on coating thickness for different capillary numbers. ——— from eq. (14), – – – from eq. (13)
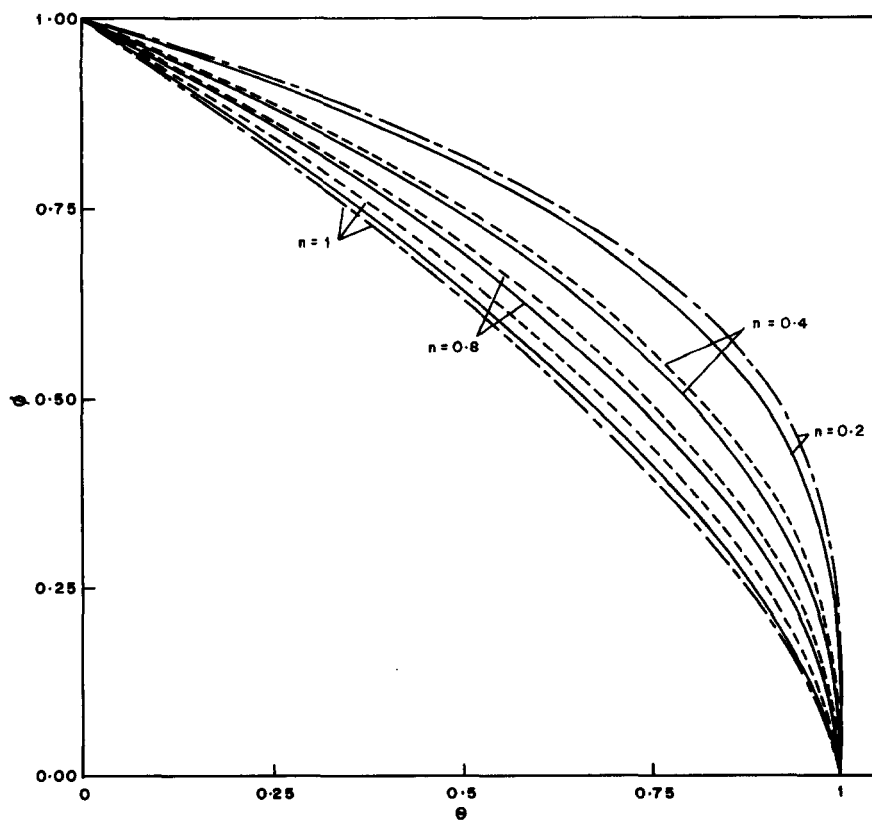

Fig. 5. Effect of slip velocity on coating thickness for various pseudoplastic liquids. ——— Ca = 0.01, – – – Ca = 1 from eq. (14); — – — from eq. (13)

6. Calculation of slip velocities from observed coating thicknesses

Eqs. (13) and (14) can be used for calculating the slip velocities. In order to do so, we shall use the data on film thickness presented by Gutfinger and Tall-madge [6]. Table 2 shows the slip velocities calculated from the experimental data. Two striking observations emerge: The first is that slip velocity increases as the polymer concentration is increased. This agrees with the observations of Metzner et al. [22] and Carreau et al. [19], who showed that stress induced diffusion increases with polymer concentration. The second striking observation is that the magnitude of slip effects are extremely large and indeed the slip velocities range from about 60% to 99% of the withdrawal velocities. That such dramatic results are possible is evident from the analysis presented by Metzner et al. [22], who show that the magnitude of the slip velocity reduces rapidly as the capillary diameter or the film thickness reduces and as the lengths over which the flow occurs, increases. In free coating operations such as the ones described here, there appear to be a tremendous opportunity for macromolecular migration to occur in view of the very small

transverse distances over which migration occurs and also the very large lengths over which coating is normally undertaken.

7. Upper and lower bound for coating thickness

Under equilibrium or steady-state conditions, the effect of stress induced diffusion is the formation of a thin solvent layer and a core of polymer concentration higher than the bulk concentration. Since pure solvent (being a homogeneous fluid) adheres to the wall, the film thickness then can be estimated from eq. (4) based on the solvent properties. This, perhaps, is somewhat of an idealized situation and may not be attainable in practice. Nevertheless, this should be the lower bound on film thickness. The upper bound, of course, is given by the film thickness calculated on the basis of no-slip. Figure 6 illustrates this behaviour

Table 2. Calculated slip velocities from experimental data [6]

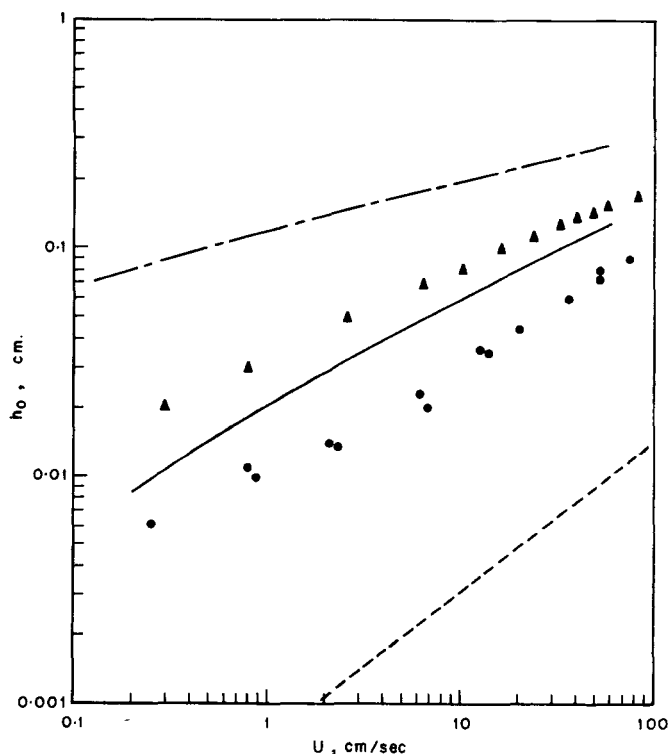| Ca	$T_{exptl.}$	$T_{calc.}$	ϕ	θ
0.16% aqueous carbopol solution, $n = 0.56$				
0.055	0.290	0.640	0.453	0.852
0.055	0.310	0.640	0.484	0.826
0.105	0.360	0.700	0.514	0.804
0.105	0.380	0.700	0.543	0.777
0.140	0.400	0.715	0.559	0.762
0.225	0.440	0.730	0.603	0.715
0.225	0.430	0.730	0.589	0.727
0.300	0.470	0.740	0.635	0.677
0.300	0.460	0.740	0.622	0.693
0.400	0.500	0.742	0.674	0.626
0.2% aqueous carbopol solution, $n = 0.308$				
0.052	0.185	0.770	0.240	0.996
0.090	0.220	0.800	0.275	0.994
0.190	0.300	0.800	0.375	0.978
0.310	0.320	0.800	0.400	0.972
0.400	0.335	0.800	0.419	0.967
0.500	0.350	0.800	0.438	0.960
0.610	0.360	0.800	0.450	0.956
0.720	0.370	0.800	0.463	0.952
0.800	0.375	0.800	0.469	0.948
0.900	0.385	0.800	0.481	0.944
1.000	0.400	0.800	0.500	0.934
1.100	0.410	0.800	0.513	0.929
1.250	0.420	0.800	0.525	0.920

Fig. 6. Upper and lower bounds on coating thickness. Experimental (6): (●) 0.16% aqueous carbopol, (▲) 0.2% aqueous carbopol [6], calculated: — — — no slip for 0.20% carbopol, ——— no slip for 0.16% carbopol, – – – no slip based on water (solvent) properties

more clearly. Experimental data for aqueous carbopol solutions are seen to be between those obtained from no-slip analysis using the solvent and solution properties. Results presented in table 3 also

Table 3. Results for cylinder withdrawal, wire radius = 0.0445 cm [14]

Liquid	h (cm)	U_c (cm/sec)	U (cm/sec)	U_w (cm/sec)	U_c/U
Newtonian					
Mineral oil	0.0051	3.53	5.6	–	0.630
	0.0270	12.11	17.2	–	0.704
	0.0651	93.01	87.3	–	1.065
	0.0840	131.40	125.4	–	1.048
Non-Newtonian					
Aqueous solutions					
0.5% CMC	0.0049	0.679	5.6	167.4	0.121
	0.0076	1.642	10.6	278.4	0.155
0.25% CMC	0.0017	0.352	5.6	37.1	0.063
	0.0023	0.673	10.6	57.5	0.063
	0.0085	7.971	36.3	350.9	0.212
0.5% Carbopol 934	0.0223	0.036	5.6	1143	0.007
	0.0263	0.052	10.6	1375	0.005
	0.0372	0.108	36.3	2005	0.003
	0.0459	0.163	87.3	2507	0.002
	0.0575	0.248	125.4	3188	0.002
0.5% Carbopol 941	0.0600	2.118	17.2	3338	0.123
	0.0775	3.336	36.3	4428	0.092
	0.0900	3.727	61.7	5264	0.064
	0.0955	4.470	87.3	5650	0.051
	0.1040	5.183	125.4	6271	0.041

corroborate this behaviour; for a given film thickness, experimental withdrawal velocity is seen to be bounded by the no-slip predictions for solution (U_c) and that for the solvent (U_w). Needless to mention that a knowledge of such bounds on film thickness for a given withdrawal velocity is of considerable practical use for design purposes.

8. Some design considerations

The evidence presented in the foregoing strongly suggests that the discrepancy between the theory and the experiment that is being observed over the last decade as regards coating of non-Newtonian fluids is concerned can be largely attributable to the slip effect. Since almost all the systems being handled for coatings would be dispersed systems, it would seem that slip effect would be a rule rather than an exception. In this event it would be useful to suggest a possible design and scale-up method which will enable a reasonable estimate of the coating thickness.

In general, the relationship between the slip velocity, u_s, and the wall shear stress can be written as

$$u_s = \beta \tau_w^a \tag{15}$$

where the parameters β and a depend on the system under consideration and therefore are to be determined experimentally. Mashelkar and Dutta [28] have performed an analysis of the experimental data on films [18, 19], from which a value of a, which is close to unity can be deduced. Eq. (15) can be combined with eqs. (11) and (14) to give

$$\phi^a \beta^* T_0^a + (\phi T_0)^{n+1} + \phi^{(1-b(1-n))/4b}(1 - T_0^{(n+1)/n})$$
$$= 1 \tag{16}$$

where

$$\beta^* = \beta \left[\frac{(\rho g)^{an} K^a}{U^{n(1-a)+1}} \right]^{1/(n+1)} . \tag{17}$$

The above is an implicit equation for the calculation of coating thickness provided the physical parameters such as ρ, g, σ, the rheological parameters such as K and n and also the slip coefficient β will be known. Note that β depends upon the type of dispersion and the concentration. The value of β can be calculated by performing experiments in a capillary tube in the range of shear stress which would be in the same range as is to be expected in the coating operations; see eq. (11).

The flow rate pressure drop relationship with a modified boundary condition for slip, as given in eq. (15), can be written as (29)

$$Q - \frac{\pi R_t^3}{\sigma_w^3} \int_0^{\sigma_w} \sigma'^2 f(\sigma') d\sigma' = \beta \sigma_w^a \qquad (18)$$

where $\sigma_w = \dfrac{\Delta P R_t}{2 L_t}$ is the wall shear stress and $f(\sigma')$ is the shear rate. The function $f(\sigma')$ can readily be obtained from viscometric (cone-and-plate) measurements. Knowing $f(\sigma')$, pressure drop flow rate data allows determination of the slip parameters β and a from eq. (18). Alternatively, these parameters can also be estimated by conducting experiments similar to those reported by Carreau et al. [19] for flow down an inclined plane. The values of β and a, thus obtained, can then be used in conjunction with eqs. (4) and (16) to obtain a reasonable estimate of the coating thickness, h_0. This would indeed be somewhat approximate, but in view of the large differences which exist between the present theories and practice, it could be a better design method than a straightforward application of existing phenomenological theories, which do not incorporate slip effects.

9. Concluding Remarks

In the foregoing, it has been argued that the reduced entrainment observed in free coating of non-Newtonian liquids is primarily due to the formation of a slip layer caused by the phenomenon of stress induced diffusion. Undoubtedly, the fluid viscoelasticity plays a role in governing the coating thickness, but it appears that it is the effective slippage of the liquid at the moving substrate that contributes predominantly in controlling it. Besides, it needs to be mentioned that even though the present work assumes a power-law model to represent the non-Newtonian behaviour, the basic methodology is a general one and can readily be employed to handle problems of coating thickness design for fluids described by any other constitutive relationship.

References

1. Landau, L., B. V. Levich, Acta Physchim. URSS 17, 41 (1942).
2. White, D. A., J. A. Tallmadge, Chem. Eng. Sci. 20, 33 (1965).
3. Spiers, R. P., C. V. Subbaraman, W. L. Wilkinson, Chem. Eng. Sci. 29, 389 (1974).
4. Soroka, A. J., J. A. Tallmadge, Amer. Inst. Chem. Eng. J. 17, 505 (1971).
5. Esmail, M. N., R. L. Hummel, Amer. Inst. Chem. Eng. J. 21, 958 (1975).
6. Gutfinger, C., J. A. Tallmadge, Amer. Inst. Chem. Eng. J. 11, 403 (1965).
7. Tallmadge, J. A., Chem. Eng. Sci. 24, 471 (1969).
8. Tallmadge, J. A., Amer. Inst. Chem. Eng. J. 16, 925 (1970).
9. Tallmadge, J. A., Amer. Inst. Chem. Eng. J. 12, 1011 (1966).
10. Spiers, R. P., C. V. Subbaraman, W. L. Wilkinson, Chem. Eng. Sci. 30, 379 (1975).
11. Hildebrand, R. E., J. A. Tallmadge, Can. J. Chem. Eng. 46, 394 (1968).
12. Groenveld, P., Chem. Eng. Sci. 25, 1579 (1970).
13. Gutfinger, C., Ph. D. Thesis, Yale University, 1965.
14. Roy, S. C., Can. J. Chem. Eng. 49, 583 (1971).
15. Tallmadge, J. A., Amer. Inst. Chem. Eng. J. 14, 837 (1968).
16. Middleman, S., Polym. Eng. Sci. 18, 355 (1978).
17. Middleman, S., Fundamentals of Polymer Processing, p. 223, McGraw-Hill (New York 1977).
18. Astarita, G., G. Marrucci, G. Palumbo, Ind. Eng. Chem. Fund. 3, 333 (1964).
19. Carreau, P. J., Q. H. Bui, P. Leroux, Rheol. Acta 18, 600 (1979).
20. Jastrzebski, Z. D., Ind. Eng. Chem. Fund. 6, 445 (1967).
21. Kozicki, W., S. N. Pasari, A. R. K. Rao, C. Tui, Chem. Eng. Sci. 25, 41 (1970).
22. Metzner, A. B., Y. Cohen, C. Rangel-Nafaile, J. Non-Newtonian Fluid Mech. 5, 449 (1979).
23. Tirrell, M., M. F. Malone, J. Polym. Sci. 15, 1569 (1977).
24. Janssen, L. P. B. M., Rheol. Acta 19, 32 (1980).
25. Fessler, J. H., A. G. Ogston, Trans. Far. Soc. 47, 667 (1951).
26. Couper, A., R. F. T. Stepto, Trans. Far. Soc. 65, 2486 (1969).
27. Kedem, O., A. Katchalsky, J. Polym. Sci. 15, 321 (1955).
28. Mashelkar, R. A., A. Dutta, Chem. Eng. Sci., in press (1982).
29. Astarita, G., G. Marrucci, Principles of Non-Newtonian Fluid Mechanics, p. 57, McGraw-Hill, (London, 1974).

Authors' address:

Dr. A. Dutta, Dr. R. A. Mashelkar
Chemical Engineering Division
* National Chemical Laboratory
Pune 411008 (India)